THE PROTEIN SOCIETY

Domain architecture of vasohibins required for their chaperone-dependent unconventional extracellular release

Tetsuya Kadonosono,[1] Wanaporn Yimchuen,[1] Takuya Tsubaki,[1] Tadashi Shiozawa,[1] Yasuhiro Suzuki,[2] Takahiro Kuchimaru,[1] Yasufumi Sato,[2] and Shinae Kizaka-Kondoh[1]*

[1]Department of Life Science and Technology, School of Life Science and Technology, Tokyo Institute of Technology, Yokohama 226-8501, Japan

[2]Department of Vascular Biology, Institute of Development, Aging, and Cancer, Tohoku University, Sendai 980-8575, Japan

Received 4 September 2016; Accepted 16 November 2016
DOI: 10.1002/pro.3089
Published online 11 February 2017 proteinscience.org

Abstract: Vasohibins (VASH1 and VASH2) are recently identified regulators of angiogenesis and cancer cell functions. They are secreted proteins without any classical secretion signal sequences, and are thought to be secreted instead via an unconventional protein secretion (UPS) pathway in a small vasohibin-binding protein (SVBP)-dependent manner. However, the precise mechanism of SVBP-dependent UPS is poorly understood. In this study, we identified a novel UPS regulatory system in which essential domain architecture (VASH-PS) of VASHs, comprising regions $VASH1_{91–180}$ and $VASH2_{80–169}$, regulate the cytosolic punctate structure formation in the absence of SVBP. We also demonstrate that SVBP form a complex with VASH1 through the $VASH1_{274–282}$ (SIa), $VASH1_{139-144}$ (SIb), and $VASH1_{133–137}$ (SIc), leading to the dispersion in the cytosol and extracellular release of VASH1. The amino acid sequences of VASH-SIa and VASH-PS, containing SIb and SIc, are highly conserved among VASH family members in vertebrates, suggesting that SVBP-dependent UPS may be common within the VASH family. This novel UPS regulatory system may open up new avenues for understanding fundamental protein secretion in vertebrates.

Keywords: unconventional protein secretion; vasohibins; molecular chaperon; punctate structure formation

Statement

Vasohibins (VASHs) are secreted via an unconventional protein secretion (UPS) pathway. In this study, we analyzed a series of deletion and substitution mutants constructed on the basis of VASH1 secondary structure and reveal that cytosolic punctate structure (PS) formation and extracellular release of VASHs are regulated by physical interaction with a chaperone protein through three conserved domains of VASHs. This novel UPS regulatory system may open up new avenues for understanding fundamental protein secretion in vertebrates.

Introduction

Vasohibin-1 (VASH1) and vasohibin-2 (VASH2) are members of the vasohibin family, a novel family of angiogenic regulators.[1–3] Spatiotemporal analyses of these genes in mice indicate that VASH1 and VASH2 have distinct expression patterns and opposing functions; VASH1 is mainly released from endothelial cells to terminate angiogenesis, while VASH2 is mainly expressed in mononuclear cells to promote angiogenesis.[4] In addition, VASH2 was found to be secreted from several types of cancer cells, including ovarian adenocarcinoma,[3] gastric cancer,[5] hepatocellular carcinoma,[6]

Grant sponsor: Grant-in-Aid for Scientific Research on Innovative Areas "Integrative Research on Cancer Microenvironment Network" from the Ministry of Education, Culture, Sports, Science and Technology of Japan; Grant number: JP22112009.

*Correspondence to: Shinae Kizaka-Kondoh, School of Life Science and Technology, Tokyo Institute of Technology, Yokohama 226-8501, Japan. E-mail: skondoh@bio.titech.ac.jp

endometrial cancer,[7] colon cancer,[8] breast cancer,[9] and pancreatic ductal adenocarcinoma,[10] where this protein acts to enhance tumor growth by promoting angiogenesis. No known functional motifs have been identified in either the VASH1 or VASH2 amino acid sequences, but order/disorder orientation analysis suggests that the N- and C-terminal disordered regions have distinct functions in both VASH1 and VASH2.[11]

Most newly synthesized secretory proteins are secreted through the conventional endoplasmic reticulum (ER)-Golgi secretory pathway, in which proteins with a signal peptide are first recognized by a signal recognition particle and allowed to enter the ER, from where they are translocated to the Golgi apparatus using vesicles covered with coat protein complex II; they are then modified and processed in the Golgi, sorted into secretory vesicles, and finally released into the extracellular space.[12,13] However, the VASHs contain no classical secretion signal sequences and are hypothesized to be released via nonconventional protein extracellular transport systems, the so-called UPS pathways, into the extracellular space.[1] So far, two types of UPS have been discovered: Interleukin (IL)−1β,[14,15] IL-33,[16] Acb1,[17–19] tissue transglutaminase,[20] galectin-3,[21] macrophage migration inhibitory factor,[22] and insulin-degrading enzyme[23] are all secreted through vesicle intermediates such as autophagosome-like vesicles, recycling endothomes, secretory lysosomes, multivesicular bodies, and exosomes, or via microvesicle shedding,[13,24] whereas proteins such as the fibroblast growth factors (FGFs) are secreted via non-vesicular translocation across the plasma membrane.[13,25] In the case of the VASHs, small vasohibin-binding protein (SVBP), a coiled-coil protein composed of 66 amino acids,[26] may be involved in the extracellular release of the VASHs, because overexpression or knockdown of SVBP has been shown to enhance or reduce VASH1 secretion, respectively.[26] However, the secretion mechanism of the VASHs via SVBP-dependent UPS is poorly understood.

Here, we suggest a regulatory system of chaperone-dependent UPS by which SVBP promotes the extracellular release of the VASHs. Notably, we demonstrate that VASHs have a unique domain architecture containing critical sequences for distinct functions: PS formation, dispersion in the cytosol, and extracellular release. SVBP regulates these functions through sequence-specific interaction with the VASHs and translocates these proteins from the cytosol into the extracellular space on cellular demand.

Results

Analysis of subcellular localization and extracellular release of VASH1 by tracking system

Fluorescence and bioluminescence are highly sensitive tools for the spatial and quantitative analyses of intracellular and extracellular proteins. To analyze the subcellular localization and extracellular secretion of VASH1, superfolder green fluorescent protein (sfGFP)[27] or *Renilla* luciferase 8.6-535 (RLuc)[28] was fused to the C-terminal end of VASH1, constructing VASH1-sfGFP or VASH1-RLuc, respectively[29] [Fig. 1(A)]. SVBP was also fluorescently visualized by fusing it with a red fluorescent protein, mRuby2[30] [SVBP-mRuby2; Fig. 1(A)]. After transient transfection of VASH1-sfGFP cDNA into HeLa cells, VASH1 was found to show cytoplasmic PS formation [Fig. 1(B)], which did not fully overlap with any organelles examined, such as ER, mitochondria, or lysosome [Fig. 1(C)]. However, when VASH1 was coexpressed with SVBP or SVBP-mRuby2, these PS were completely absent and VASH1 was dispersed throughout the cytosol [Fig. 1(B)]. In our previous report, SVBP was shown to stabilize VASH1 by increasing its solubility and inhibiting ubiquitination in the cytosol, eventually enhancing VASH1 extracellular release.[26] Thus, we evaluated the level of VASH1 protein in both the culture medium and the cell lysate by measuring bioluminescence after coexpression of VASH1-RLuc and SVBP. In the presence of SVBP, VASH-1 fused to RLuc at the C-terminal end (VASH1-RLuc) significantly increase RLuc activity in the medium while VASH-1 fused to RLuc at the N-terminal end [RLuc-VASH1; Fig. 1(A)] and RLuc alone did not [Fig. 1(D)]. Furthermore, the fusion of sfGFP to the N-terminal end of VASH1 [sfGFP-VASH1; Fig. 1(A)] led to the PS formation regardless of co-expression of SVBP [Fig. 1(E)]. These results demonstrate that N-terminal structure of VASH1 is important for SVBP-dependent dispersion in the cytosol and extracellular release and that the fusion of reporter proteins to the C-terminus successfully track the intracellular behavior of VASH1, revealing that VASH1 intrinsically shows PS formation in cells and that SVBP inhibits this PS formation and enhances extracellular release of VASH1.

Determination of the domain necessary for PS formation in VASHs

We hypothesized that VASH1 has domain architecture that facilitates the PS formation, and that SVBP can inhibit this PS formation by specific protein-protein interactions with VASH1, thereby enhancing the extracellular release of VASH1. To verify this hypothesis, we first identified the domain necessary for formation of PS within the VASH1 sequence (VASH1-PS). The cDNAs of various VASH1 deletion mutants, D1 (1–344), D2 (1–300), D3 (1–270), D4 (1–160), D5 (1–90), D6 (331–365), D7 (301–365), D8 (271–365), D9 (91–270), and D10 (91–180) [Fig. 2(A)], were fused to sfGFP cDNA and transiently introduced into HeLa cells. After 48 h, localization of the fusion proteins was observed with fluorescence microscopy [Fig. 2(B)]. The D1, D2, D3, D9, and D10 mutant proteins formed clear PS while

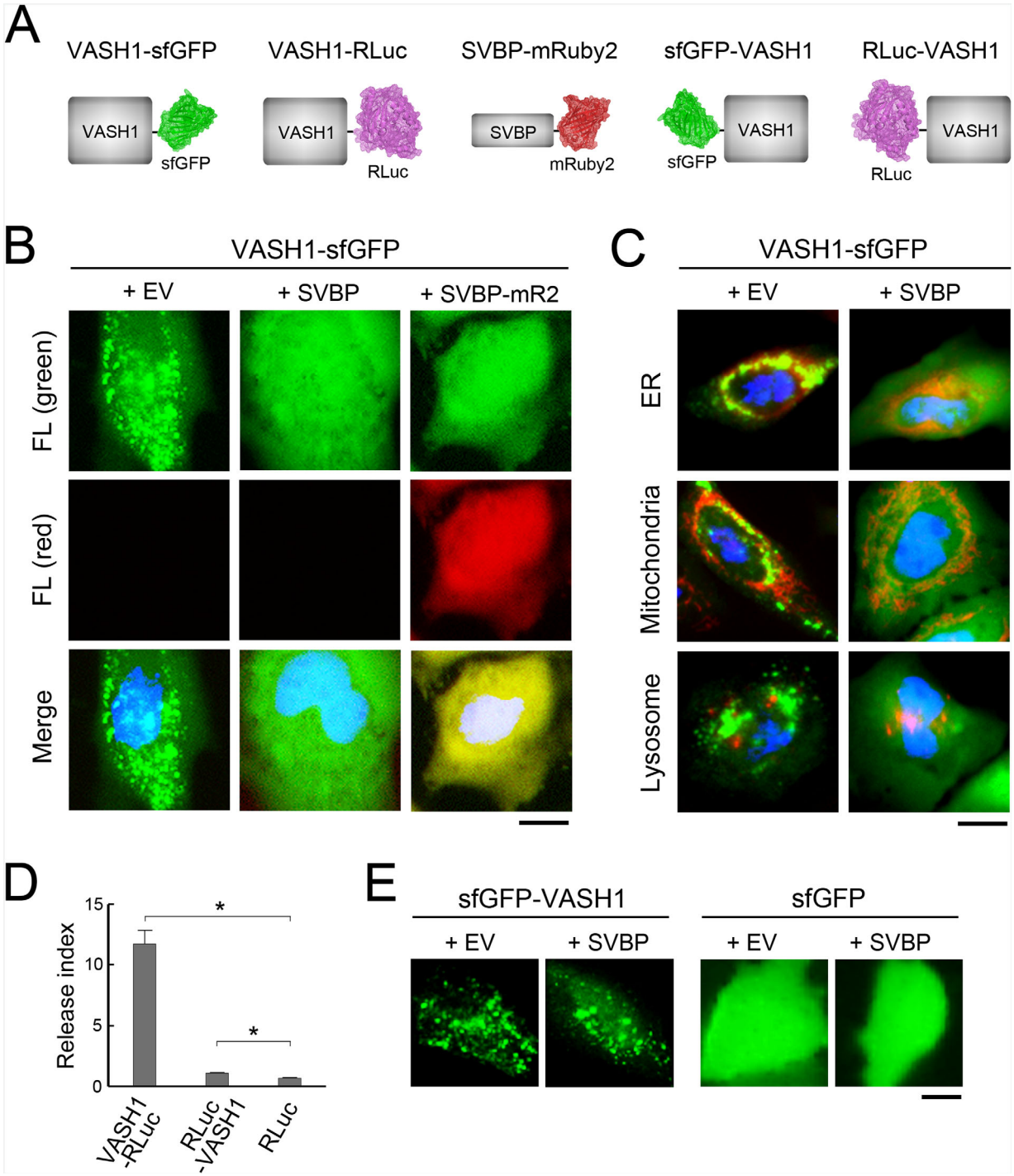

Figure 1. VASH1-reporting systems. A: Schematic diagrams of VASH1 fusion proteins. Green fluorescent protein sfGFP and bioluminescent enzyme RLuc were each genetically ligated to the C-terminal (VASH1-sfGFP and VASH1-RLuc) or N-terminal (sfGFP-VASH1 and RLuc-VASH1) of VASH1. Red fluorescent protein mRuby2 was ligated to the C-terminal of SVBP. B: Fluorescence micrographs of HeLa cells cotransfected with VASH1-sfGFP-encoding vector and empty (EV), SVBP-encoding or SVBP-mRuby2-encoding (SVBP-mR2) vectors. Nuclei were stained with Hoechst 33342 (blue) and merged images of all colors are shown in the bottom panels. Bar = 10 μm. C: Merged fluorescence micrographs of HeLa cells cotransfected with VASH1-sfGFP-encoding vector and empty (EV) or SVBP-encoding vectors. Nuclei and ER, mitochondria, or lysosome were stained with Hoechst 33342 (blue) and ER-ID (red), MitoTracker (red), or LysoTracker (red), respectively. Bar = 10 μm. D: SVBP-dependent release of VASH1-RLuc, RLuc-VASH1, and RLuc from the cells. Release index was calculated as in methods section. Mean ± S.E.M. of four independent experiments is shown. (*$P < 0.005$). E: Fluorescence micrographs of HeLa cells cotransfected with sfGFP-VASH1-encoding or sfGFP-encoding vectors and empty (EV) or SVBP-encoding vectors. Bar = 10 μm.

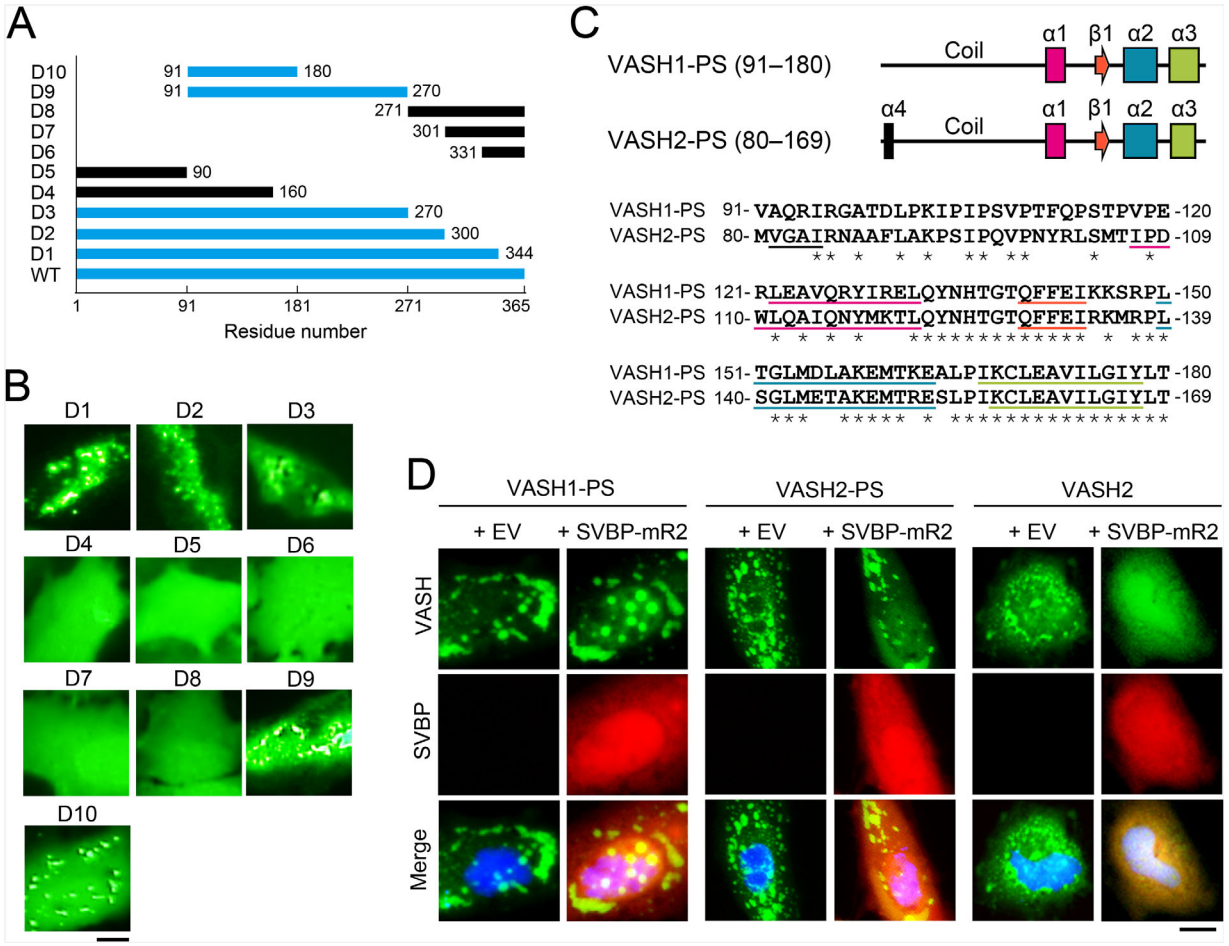

Figure 2. Determination of the domain necessary for PS formation in VASHs. A: Summary of mutant VASH1 D1–D10. The sfGFP-fused mutants that formed PS in HeLa cells are colored in blue. B: Fluorescence micrographs of HeLa cells transfected with mutant VASH1-sfGFP-encoding vectors. C: Diagram of predicted secondary structures and alignment of sequences of VASH1-PS and VASH2-PS. Amino acid sequences predicted to form α-helix-1, β-sheet-1, α-helix-2, α-helix-3, and α-helix-4 are indicated by magenta, orange, blue, green, and black underlines, respectively. *: Identical amino acids shared by VASH1-PS and VASH2-PS. D: Fluorescence micrographs of HeLa cells cotransfected with VASH1-PS-sfGFP-encoding (VASH1-PS), VASH2-PS-sfGFP-encoding (VASH2-PS), or VASH2-sfGFP-encoding (VASH2) vectors and empty (EV) or SVBP-mRuby2-encoding (SVBP-mR2) vectors. Nuclei were stained with Hoechst 33342 (blue) and merged images of all colors are shown in the bottom panels. Bar = 10 μm.

the D4, D5, D6, D7, and D8 mutant proteins formed no visible PS in the cells, indicating that the region comprising amino acid residues 91–180 contains VASH1-PS.

Human VASH2 (355 amino acid residues), a member of vasohibin family, has 52.5% amino acid sequence homology with human VASH1 (365 amino acid residues),[11] suggesting that a corresponding domain to VASH1-PS similarly facilitates the PS formation of VASH2 in the cytosol. Sequence alignment using ClustalW[31] revealed that the VASH2 sequence 80–169 corresponded to the VASH1-PS with 63.3% homology [Fig. 2(C)]. Furthermore, its secondary structure as predicted with the PSIPRED program[32] revealed that VASH1-PS and VASH2-PS have conserved amino acid compositions of 100% for β-sheet 1 and α-helix 3, 71.4% for α-helix 2, 45.5% for α-helix 1, and 35.5% for the random coil [Fig. 2(C)], suggesting the importance of secondary structure in this domain. To examine whether VASH1-PS and VASH2-PS have the same function in cytosolic PS formation, VASH1-PS and VASH2-PS was expressed as a fusion protein with sfGFP in HeLa cells and its intracellular localization was observed with fluorescence microscopy [Fig. 2(D)]. The result showed that both VASH1-PS-sfGFP and VASH2-PS-sfGFP formed PS within the cells, confirming the common PS domain function in the VASHs. Notably, coexpression of VASH1-PS-sfGFP or VASH2-PS-sfGFP with SVBP-mRuby2 also exhibited PS formation within the cells, confirming that the PS domain alone cannot facilitate SVBP-dependent dispersion in the cytosol.

Analysis of domain architecture of VASH1-PS

To further analyze VASH1-PS, we designed the next set of deletion mutants based on the secondary

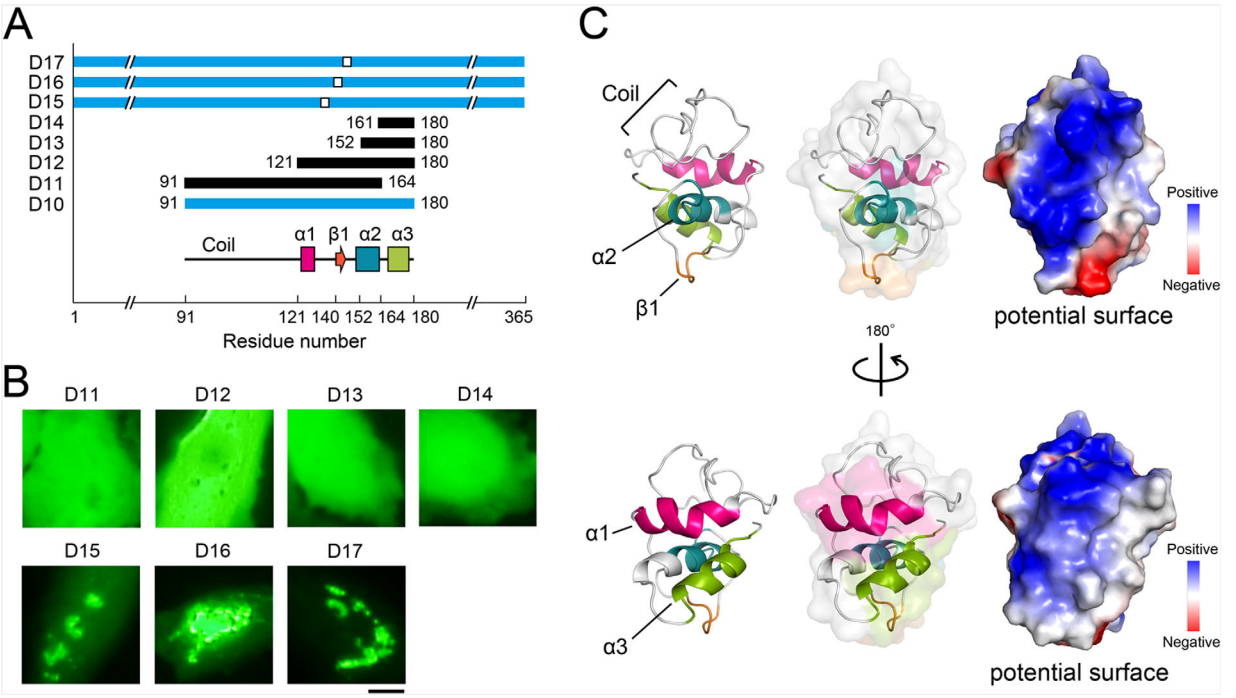

Figure 3. Analysis of domain architecture of VASH1-PS. A: Summary of mutant VASH1 D10–D17. The sfGFP-fused mutants that formed PS in HeLa cells are colored in blue. The alanine substitution regions in D15, D16, and D17 are represented with open boxes. The predicted secondary structures within VASH1-PS are also shown as Figure 2(C). B: Fluorescence micrographs of HeLa cells transfected with mutant VASH1-sfGFP-encoding vectors are shown. Bar = 10 μm. C: Representative surface structures and potential of VASH1-PS during 5.0–10.0 ns trajectories. In the surface structures of VASH1-PS, the coil, α1, β1, α2, and α3 domains are highlighted in gray, magenta, orange, blue, and green, respectively. In the potential interacting surfaces, the positively charged and negatively charged regions are indicated in blue and red, respectively.

structure, D11–D17. D11 (91–164, Δα3), D12 (121–180, Δcoil), D13 (152–180, Δcoil, α1, β1), and D14 (161–180, Δcoil, α1, β1, α2) [Fig. 3(A)] and constructed plasmids expressing these mutants as fusion proteins with sfGFP. Transient expression of these mutants in HeLa cells exhibited that none of the mutant proteins formed any PS [Fig. 3(B)], indicating that both the random coil (91–120) and α-helix 3 (165–180) are necessary for PS formation. In contrast, alanine-substituted mutants within the β-sheet 1 region, D15 (133–137A), D16 (139–144A), and D17 (145–149A) [Fig. 3(A)], formed PS [Fig. 3(B)], indicating that these regions are not required for PS formation. These results confirmed that the amino acid sequence 91–180 is necessary and sufficient for VASH1-PS, in which several essential domains for PS formation are connected via nonessential spacer sequence.

To understand the mechanism underlying PS formation of VASH1, we carried out *in silico* predictions of the surfaces of VASHs-PS with 10 ns molecular dynamic (MD) simulations. The 5.0–10.0 ns trajectories of VASH1-PS revealed that the coil and α-helix 2 are likely to form a positively charged anterior surface and that the α-helixes 1 and 3 compose hydrophobic posterior surface [Fig. 3(C)], suggesting that these deviations of surface potential in VASH1-PS contribute to PS formation.

Identification of motifs in VASH1 necessary for the SVBP-dependent cytosolic dispersion and extracellular release

To identify the amino acid sequences in VASH1 necessary for its SVBP-dependent dispersion in the cytosol, the mutant containing intact VASH1-PS and thus showing PS formation in the cytosol (D1, D2, D3, D9, D10, D15, D16, and D17 in Figs. 2 and 3) were coexpressed with SVBP in HeLa cells and their intracellular localization was observed [Fig. 4(A)]. Although D2 was distributed throughout the cell, D3 showed PS formation regardless of coexpression with SVBP, indicating the involvement of the 271–300 sequence in the SVBP-dependent dispersion in the cytosol. To further narrow down the sequence required for SVBP-dependent dispersion of VASH1, D18 (274-282A), an alanine-substitution mutant in the 274-282 sequence (SIa), was constructed [Fig. 4(B)] and coexpressed with SVBP in HeLa cells. In this case, the SVBP-dependent cytosolic dispersion was not observed, revealing that SIa is essential for this event [Fig. 4(C)]. In addition, among the alanine-substitution mutants (D15, D16, and D17) in PS domain, D15 and D17 showed SVBP-dependent cytosolic dispersion, while D16 did not, indicating that the 139–144 sequence (SIb) is also crucial for SVBP-dependent dispersion in the cytosol [Fig. 4(A)]. These results suggest that D15 and D17 may interact with SVBP but

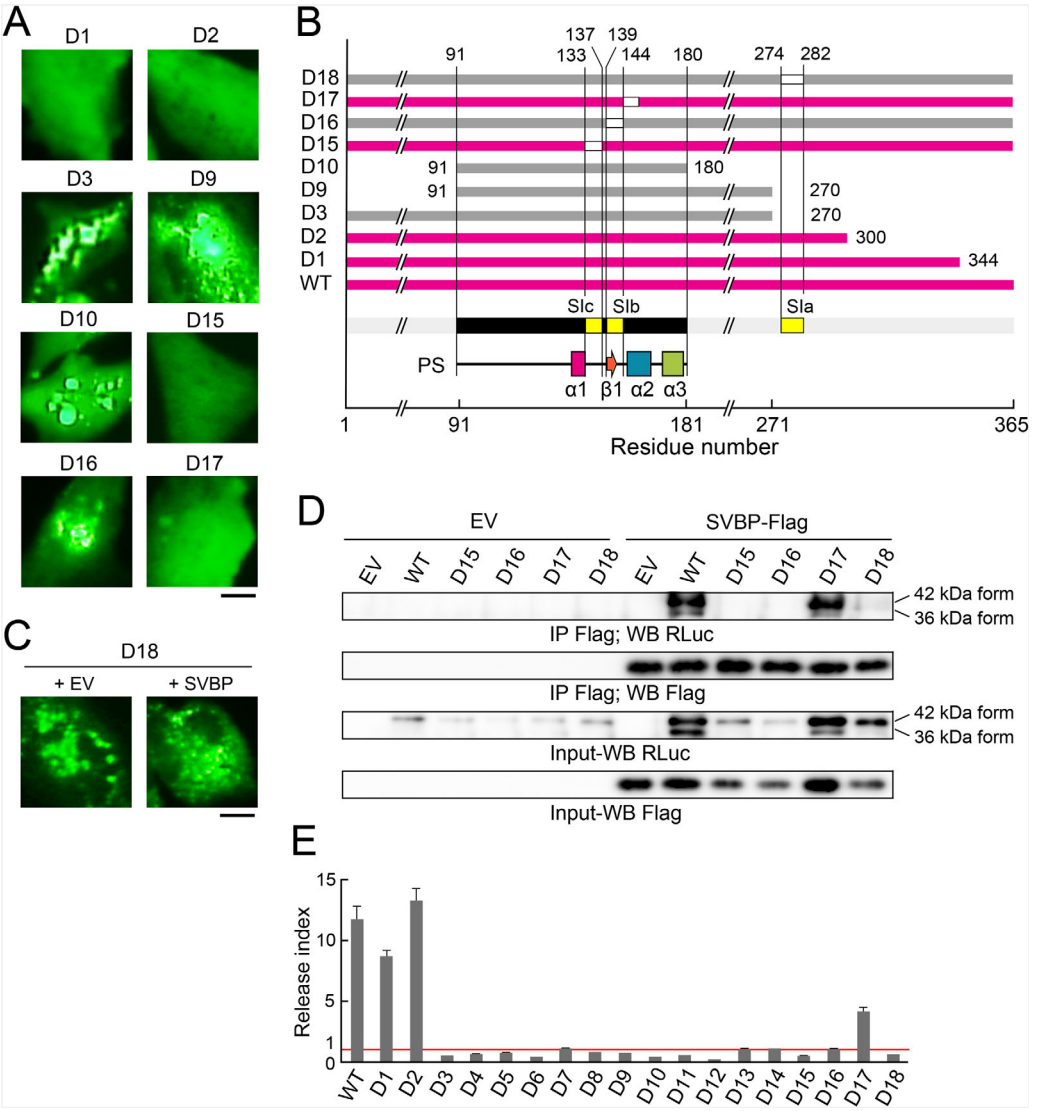

Figure 4. Identification of sequences in VASH1 necessary for the SVBP-dependent whole cell distribution and extracellular-release. A: Fluorescence micrographs of HeLa cells cotransfected with mutant VASH1-sfGFP-encoding and SVBP-encoding vectors. Bar = 10 μm. B: Summary of VASH1 D1, D2, D3, D9, D10, D15, D16, D17, and D18 mutant proteins. The sfGFP-fused mutants that distributed throughout the cells when coexpressed with SVBP, are colored in magenta. The alanine substitution regions in D15, D16, and D17 are represented with open boxes. The predicted secondary structures within VASH1-PS are shown as Figure 2(C) and motifs necessary for PS formation (closed bar), SVBP interaction (SIa and SIb, yellow boxes) and extracellular release (SIc, yellow box) are also shown. C: Fluorescence micrographs of HeLa cells cotransfected with D18-sfGFP-encoding vectors (D18) and empty (EV) or SVBP-encoding vectors. Bar = 10 μm. D: Immunoprecipitation of the VASH1–SVBP protein complex. Cell lysate from HeLa cells cotransfected with VASH1-RLuc-encoding (WT), D15-RLuc-encoding (D15), D16-RLuc-encoding (D16), D17-RLuc-encoding (D17), D18-RLuc-encoding (D18), or empty (EV) vectors and SVBP-Flag-encoding or empty (EV) vectors were immunoprecipitated with anti-Flag antibody. Immunoprecipitates were analyzed by Western blotting using anti-RLuc antibody. E: SVBP-dependent extracellular release of mutant VASH1-RLuc. Release index was calculated as described in methods section. Mean ± S.E.M. of four independent experiments is shown. Red line indicates release index = 1.

D16 and D18 may not. To investigate the interaction between these mutants and SVBP, immunoprecipitation analysis was applied for these mutants and revealed that wild type VASH1 and D17 formed a complex with SVBP but neither D15, D16, nor D18 could [Fig. 4(D)]. These results indicate that in addition to SIa and SIb, sequence 133–137 (SIc) in PS domain is essential for the VASH1-SVBP complex formation and suggest that SIa and SIb are enough and necessary for interaction with SVBP to inhibit PS formation but not enough to make a tight complex formation.

To determine the causal relationships among cytosolic dispersion, the tight complex formation with SVBP, and extracellular release of VASH1, mutant proteins were fused to RLuc and expressed with SVBP in HeLa cells, followed by the measurement of the

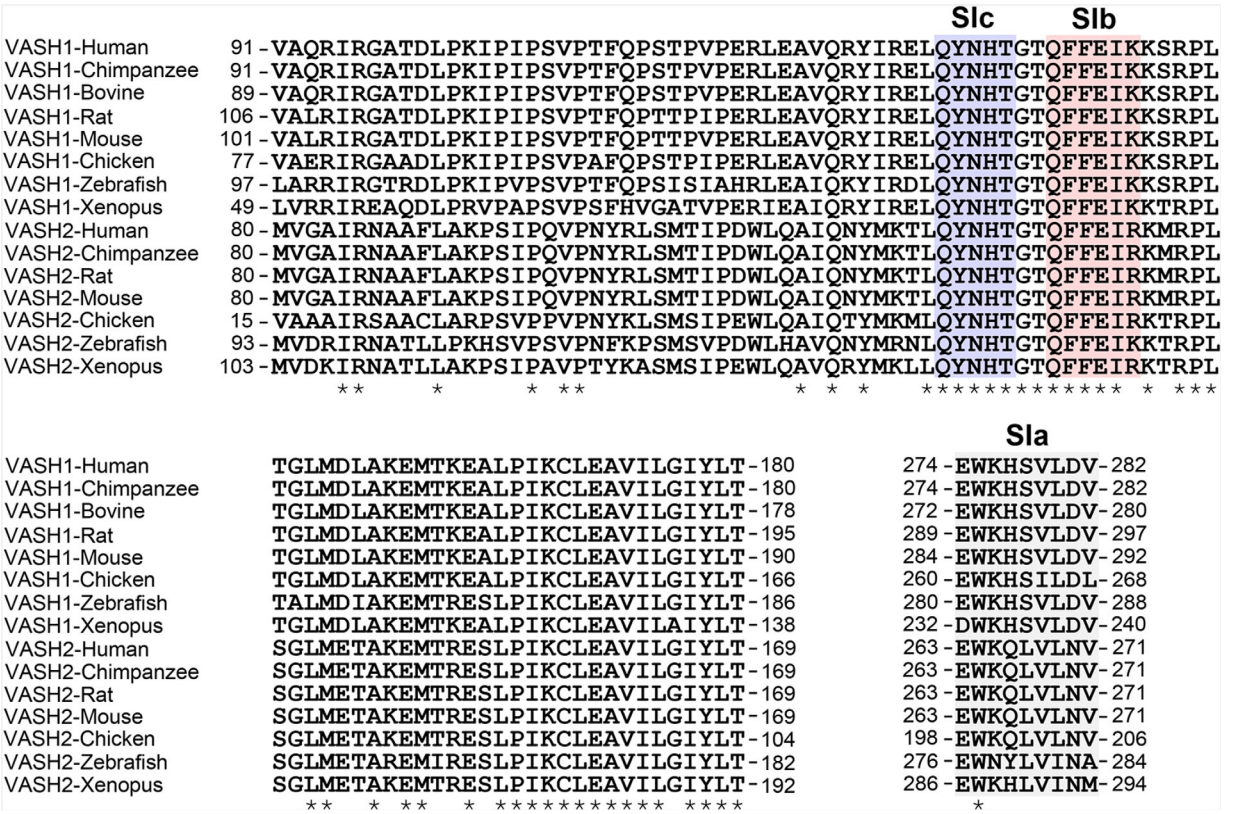

Figure 5. Multiple sequence alignment of VASH-PS and VASH-SIa. Amino acid sequences of VASH-PS and VASH-SIa of VASH family proteins in the vertebrates (except for reptiles) were analyzed for homology. *: Identical amino acid sequence shared among these species.

luciferase activities [Fig. 4(E)]. After 48 h incubation, we found that the extracellular release of the mutants that lacked either SIa or SIb (D3, D4, D5, D6, D7, D8, D9, D10, D11, D12, D13, D14, D16, and D18) was not enhanced by SVBP [Fig. 4(E)]. In contrast, the mutants having intact SIa and SIb (D1, D2, and D17) were increased in SVBP-dependent release from the cells, except for the D15 mutant [Fig. 4(E)], which lacks SIc [Fig. 4(B)]. SIc was required for the tight complex formation with SVBP as shown by fail of complex formation between SVBP and D15 mutant harboring alanine-substitution in SIc [Fig. 4(D)], suggesting the importance of the strong binding between VASH1 and SVBP for extracellular release. The D1, D2, and D17 mutants, which all contain SIa, SIb, and SIc, successfully exhibited SVBP-dependent extracellular release as indicated by the significantly high luciferase activity in their culture media.

Conservation of VASH-PS and SIa amino acid sequences among VASH family

Human VASH1-PS is highly conserved across the vertebrates except for reptiles (100% for chimpanzee, 100% for bovine, 97% for rat, 98% for mouse, 96% for chicken, 81% for zebrafish, and 80% for *Xenopus*). Notably, SIb and SIc are highly conserved and tryptophan residue within SIa is perfectly matched among these species (Fig. 5). These results support the hypothesis that all three motifs, SIa, SIb, and SIc, play important roles in SVBP-dependent UPS of VASHs.

Discussion

In this study, we successfully demonstrated a novel UPS regulatory system, SVBP-dependent extracellular release of VASH1, by identifying the contributing small-domain architectures, SIa (274-EWKHSVLDV-282), SIb (139-QFFEIK-144) and SIc (133-QYNHT-137): SIa, SIb, and SIc are necessary for a physical association with SVBP and the extracellular release of VASH1 (Fig. 4). These motifs are highly conserved among VASH family members in the vertebrates (Fig. 5), strongly suggesting that VASH proteins uses the same secretion mechanism as VASH1, while opposite function between VASH1 and VASH2 may be due to their disordered regions in the N- and C-termini.

To understand the VASHs' UPS, we constructed a series of VASH1 mutants and analyzed their behavior by fluorescence- and luciferase-reporter tracking systems (summarized in Table I). The results suggest that VASH's UPS are controlled by SVBP through two distinct regulations. The first regulation is PS formation. In the absence of SVBP, VASHs form PS in the cytosol and thus their secretion is suppressed. Mutants' analysis revealed that

Table I. *Relationship between Status of Domain Architecture and SVBP-Dependent Extracellular Release*

	Domain architecture				Steps of SVBP-dependent extracellular release			
VASH1/ mutants	PS	SIa	SIb	SIc	PS formation without SVBP	SVBP-dependent cytosolic dispersion	Complex formation with SVBP	SVBP-dependent extracellular release
WT	○	○	○	○	+	+	+	+
D1	○	○	○	○	+	+	/	+
D2	○	○	○	○	+	+	/	+
D3	○		○	○	+	−	/	−
D4			○	○	−	/	/	−
D5					−	/	/	−
D6					−	/	/	−
D7					−	/	/	−
D8		○			−	/	/	−
D9	○		○	○	+	−	/	−
D10	○		○	○	+	−	/	−
D11			○	○	−	/	/	−
D12			○	○	−	/	/	−
D13					−	/	/	−
D14					−	/	/	−
D15	○	○	○		+	+	−	−
D16	○	○		○	+	−	−	−
D17	○	○	○	○	+	+	+	+
D18	○		○	○	+	−	−	−

○, intact; +, positive response; −, negative response; /, not done.

VASH1-PS (sequence 91–180 of VASH1, Figs. 1–3) and VASH2-PS (sequence 80–169 of VASH2, Fig. 2) are crucial elements for the PS formation of these proteins in the cytosol. Because predictive structures of VASH1-PS based on the MD simulations revealed that the positively charged anterior is exposed on the surface [Fig. 3(C)] and because amphipathic peptides such as MPG and Pep-1, which are composed of positively charged and hydrophobic amino acids, have been known to associate rapidly with oligonucleotides and polypeptides through noncovalent electrostatic or hydrophobic interactions and to form stable complexes with them,[33] we have proposed a possible mechanism showing PS formation of VASHs in the cytosol: VASH1-PS may directly form complexes with oligonucleotides and polypeptides in the cytosol via its positively charged anterior surface. In addition, positively charged proteins can bind to negatively charged anionic lipids such as phosphatidylglycerol, phosphatidylserine, phosphatidic acid, and phosphatidylinositol,[34] suggesting that VASH1-PS may bind anionic lipids within some membrane structures to form PS in the cytosol. What VASH-PS is bound to in the cytosol is under investigation but membranes of the ER, mitochondria and lysosome may not become candidates because the PS did not fully overlap with them [Fig. 1(C)].

The second regulation is tight complex formation with SVBP. Coexpression of SVBP with VASH1 completely inhibits VASH1 PS formation and facilitates its secretion [Figs. 1(D) and 4]. VASH1 mutants lacking either SIa or SIb motif (D16 and D18), which are not able to form a complex with SVBP, exhibited PS even when SVBP was coexpressed (Fig. 4), indicating that the complex formation through SIa and SIb motifs is essential for SVBP-dependent dispersion in the cytosol and extracellular release. The requirement of complex formation with SVBP for VASH-extracellular release is exhibited by the VASH1-PS mutants with an intact SIc (D4, D11, and D12), which were able to disperse in the cytosol regardless of SVBP expression (Figs. 2 and 3), but failed to be released into the extracellular space (Fig. 4) and a substitution mutation in SIc (D15), which dispersed in the cytosol in the presence of SVBP but failed to be released due to inability to form a tight complex with SVBP (Fig. 4).

From these results, we propose a SVBP-dependent UPS pathway of the VASHs (Fig. 6). VASHs intrinsically form PS probably through binding to unknown targets in the cytosol via positively charged sequences in their PS domain [Fig. 6-a], and upon secretory stimulation SVBP enhances the UPS of VASHs via two chaperone functions in the cytosol: SVBP inhibits the PS formation of VASHs by forming a tight complex via SI motifs, leading to dispersion of VASHs in the cytosol [Fig. 6-b, 6-c], and then interact with the plasma membrane [Fig. 6-d], resulting in their release into the extracellular space via an unknown mechanism [Fig. 6-e]. This process may be involved in as yet undefined pathways, which include vesicle intermediates and direct export.

We previously reported that the full-length VASH1 protein (44 kDa) is post-translationally processed, resulting in at least three smaller forms (42, 36, and 27 kDa)[35] and also that the 42 kDa (sequence 30–365) protein was mainly detected in

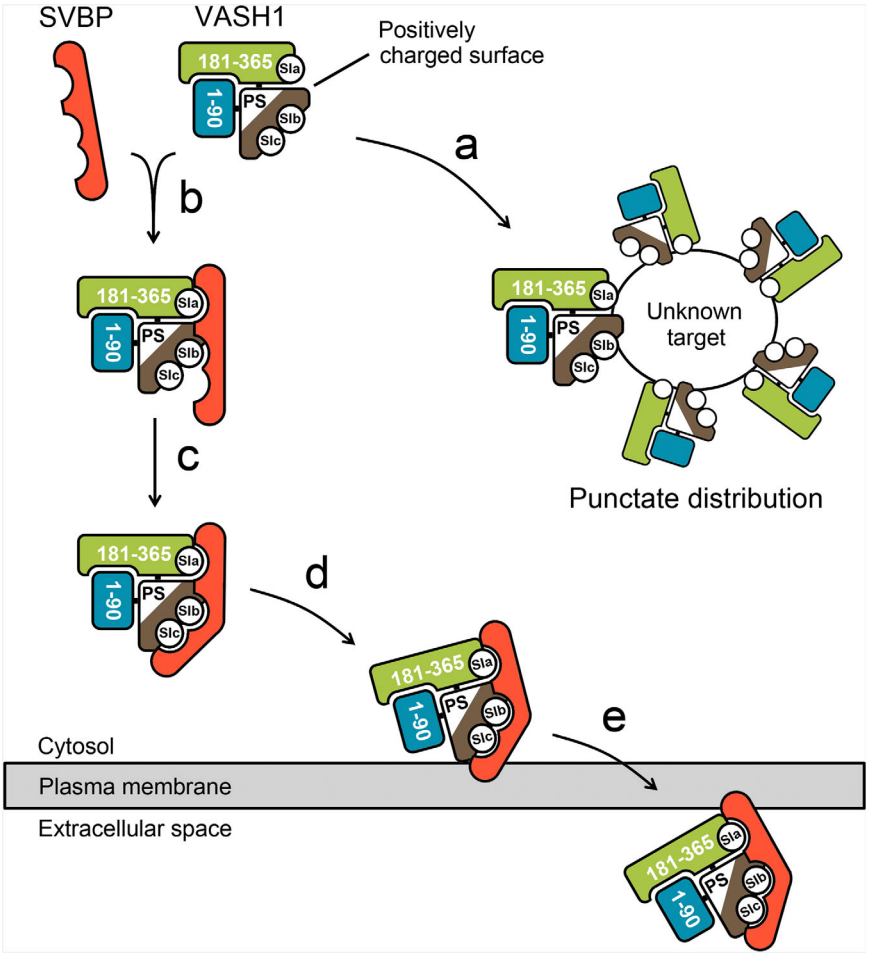

Figure 6. Hypothetical UPS pathway of the VASHs. In the absence of SVBP, VASHs form PS through positively charged surface of PS to unknown targets in the cytosol (a). When SVBP is expressed, it binds to VASHs-SIa and SIb (b) and inhibits the PS formation. VASH-SIc reinforces the binding between SVBP and VASH (c) and SVBP-VASH complexes distribute throughout the cytosol, following which they interact with plasma membrane (d) and are secreted into the extracellular space (e).

the cytosol, whereas the 36 kDa (sequence 77–365) and 27 kDa (sequence 77–318) proteins were extensively secreted in the presence of SVBP.[26] All secretable truncated forms contain VASH1-PS and VASH1-SIa, supporting the critical importance of this domain architecture for their secretion. Although the extracellular release of the truncated 42 and 36 kDa protein are easily evaluated using cells expressing VASH1-sfGFP and -RLuc, we are not able to detect the truncated 27 kDa protein, which lacks C-terminal region of VASH1. However, D2 (1–300) shows SVBP-dependent extracellular release, suggesting that truncated C-terminal region (319–365) of 27 kDa protein has few functions on the extracellular release.

IL-1β, one of the major inflammatory factors known to be secreted through UPS, is secreted via secretory vesicle intermediates.[15] However, in our study, no vesicle-like structures were observed when VASH1-sfGFP was coexpressed with SVBP in the cells (Fig. 1), indicating that the UPS of VASHs may not be mediated by vesicular translocation across the plasma membrane, similarly to the FGFs.[13] During the UPS of FGF2, its attachment to the plasma membrane through the binding of PtdIns(4,5)P_2 was proposed as the first essential step, followed by the insertion of FGF2 oligomers into the membrane-spanning hydrophilic pore and externalization by the binding of membrane-proximal heparin sulfate proteoglycans on the extracellular surface of the plasma membrane.[13,25,36] VASHs use a novel UPS mechanism by binding to SVBP that has a coiled-coil structure similar to the membrane-anchoring proteins such as the golgin proteins, which function in the conventional protein secretion system,[37,38] suggesting that SVBP may recruit VASHs into the plasma membrane. The VASH-SVBP complexes possibly then penetrate the plasma membrane through their positively charged molecular surface, as cationic proteins and peptides have been similarly observed to penetrate mammalian cells.[33,39] Further study should reveal the precise molecular mechanism of SVBP-mediated UPS of the VASHs.

Vertebrates have highly specialized blood cells such as erythrocytes, thrombocytes and leukocytes,[40] and control vascular homeostasis with a sophisticated vascular network. VASH1-PS is highly conserved among the vertebrates including humans (Fig. 5), suggesting that

SVBP-dependent UPS may be a fundamental cellular mechanism for controlling vascular homeostasis. Considering the multiple regulatory levels of the VASHs including in terms of mRNA expression level,[1,41] miR-200b-dependent mRNA silencing,[3] and ubiquitin-dependent protein degradation,[26] SVBP-dependent UPS might have evolved to prevent the unnecessary secretion of VASHs from cells and to maintain the delicate balance between proangiogenic and antiangiogenic activities in the vascular network of vertebrates.

Materials and Methods

Human cell line and culture conditions

The human cervical cancer cell line HeLa was purchased from the American Type Culture Collection (Manassas, VA) and maintained at 37°C in 5% FBS Dulbecco's Modified Eagle's Medium (Thermo Fisher Scientific, Waltham, MA) supplemented with 100 units/mL penicillin and 100 μg/mL streptomycin (Nacalai Tesque, Kyoto, Japan).

Plasmid construction for recombinant VASH1, VASH2, SVBP, and mutant proteins

The cDNAs encoding the wild-type and D1–D18 mutant VASH1 proteins each fused with sfGFP or RLuc were inserted into the EcoRV site of the pcDNA3.1 plasmid (Thermo Fisher Scientific). The cDNAs encoding full-length VASH2 or domain for the PS formation of VASH2 (residues 80–169) fused with sfGFP and for SVBP fused with mRuby2 were also inserted into the EcoRV site of separate pcDNA3.1 plasmids.

Intracellular localization of VASH1, VASH2, SVBP, and mutant proteins

The plasmids for the expression of wild-type and mutant VASH1 or VASH2 fused with sfGFP (0.125 μg each) were co-transfected with 0.125 μg of p3×FLAG-SVBP, the plasmid for the expression of SVBP-mRuby2 fusion protein, or empty pcDNA3.1 vector, into HeLa cells in 24-well plates (5.0×10^4 cells/well in 1 mL medium) and the cells were incubated for 48 h at 37°C. For nuclear staining, 1 μg Hoechst 33342 (Dojindo Laboratories, Kumamoto, Japan) was added into the culture medium 10 min before observation. For ER staining, ER-ID Red Assay Kit (Enzo Life Sciences, NY) was used according to the manufactures instruction. For mitochondria or lysosome staining, 50 n*M* MitoTracker Red (Thermo Fisher Scientific) or 75 n*M* LysoTracker Red (Thermo Fisher Scientific) were added into the culture medium 15 or 30 min before observation, respectively. Fluorescent micrographs were obtained with a Biorevo BZ-X710 fluorescence microscope (Keyence, Osaka, Japan) with the appropriate filters (Ex/Em = 470 ± 40 nm/520 ± 50 nm for sfGFP, Ex/Em = 545 ± 25 nm/605 ± 70 nm for mRuby2, ER-ID, MitoTracker, and LysoTracker, and Ex/Em = 360 ± 40 nm/460 ± 50 nm for Hoechst 33342).

Luciferase release assay

The plasmids for the expression of RLuc, wild-type VASH1 fused with RLuc, and mutant VASH1 fused with RLuc (0.125 μg each) were cotransfected with 0.125 μg of p3×FLAG-SVBP or empty pcDNA3.1 vector, into HeLa cells in 24-well plates (5.0×10^4 cells/well in 1 mL medium) and the cells were incubated for 48 h at 37°C. Luciferase activity (RLU) in the medium or in the cell lysates from each culture was determined after reaction with the RLuc substrate coelenterazine-h (10 ng/μL in PBS; Promega, Fitchburg, WI) with a GL-220 luminometer (Microtec, Chiba, Japan). The rate of extracellular release and SVBP-dependent release of RLuc, wild-type VASH1-RLuc, and mutant VASH1-RLuc (Release rate and release index) were calculated from eq 1 and 2, respectively

$$\text{Release rate} = [\text{BL}]_\text{m} / \left([\text{BL}]_\text{m} + [\text{BL}]_\text{l}\right) \quad (1)$$

$$\text{Release index} = [\text{Release rate}]_\text{S} / [\text{Release rate}]_\text{E} \quad (2)$$

where $[\text{BL}]_\text{m}$ and $[\text{BL}]_\text{l}$ indicate luciferase activities in the medium and total cell lysate, respectively, and $[\text{Release rate}]_\text{S}$ or $[\text{Release rate}]_\text{E}$ indicates release rate of cells cotransfected with SVBP encoding or empty vectors, respectively. Experiments were performed in quadruplicate, and data are represented as the mean ± standard error of the mean.

Immunoprecipitation

The plasmids for the expression of VASH1-RLuc, D15-RLuc, D16-RLuc, D17-RLuc, D18-RLuc, or empty pcDNA3.1 vector (2.5 μg each) were cotransfected with 2.5 μg of p3×FLAG-SVBP or empty pcDNA3.1 vector, into HeLa cells in 10-cm dishes (1.0×10^6 cells/dish in 10 mL medium) and the cells were incubated for 48 h at 37°C. Cells were lysed in the buffer consisting of 20 m*M* Tris-HCl (pH 8.0), 137 m*M* NaCl, 2 m*M* EDTA, and 1% Triton X-100. Cell extracts were placed on ice for 15 min and then centrifuged at 12,000*g* for 10 min to collect the supernatant. The cell lysate was incubated with mouse monoclonal anti-Flag antibody (catalogue no. F3165, Sigma-Aldrich, St. Louis, MO) for 1 h at 4°C and then protein G sepharose beads (GE Healthcare, Little Chalfont, United Kingdom) for another 1 h at 4°C. The beads were washed three times with the lysis buffer and then immunoprecipitated proteins were eluted into Laemmli sample buffer. The protein samples were separated on 12.5% SDS-polyacrylamide gel and transferred to Hybond ECL membranes (GE Healthcare). VASH1-RLuc and SVBP-Flag were detected with rabbit polyclonal anti-*Renilla* luciferase antibody (catalogue no. PM047,

Medical and Biological Laboratories, Aichi, Japan) and mouse monoclonal anti-Flag antibody (Sigma-Aldrich), respectively. Appropriate horseradish peroxidase-conjugated secondary antibodies were obtained from CST.

MD simulations

The initial coordinates for $VASH1_{91–180}$ were generated from the arylamine N-acetyltransferase 3 (NAT3) structure (PDB ID code: 4DMO), which was previously proposed to be a protein of vasohibin-like family.[42] The secondary structures of $VASH1_{91–180}$ were deployed to the corresponding positions of $NAT3_{1–80}$. The system was optimized via energy minimization, and equilibrated with backbone restraints. Then 10.0 ns production run was performed for trajectory analysis using the Amber 14 program on TSUBAME (Global Scientific Information and Computing Center, Tokyo Institute of Technology). The parameters for the MD simulations were force field = Amber ff14SB, solvent model = GB/SA, time step = 2 fs with the SHAKE algorithm, non-bonded cutoff = 999.9 Å, and temperature = 300 K using the Berendsen rescaling method.

Statistical analyses

Statistical analyses were carried out with the Student's t-test. Values of $P < 0.005$ were considered statistically significant.

Conflict of Interest

No potential conflicts of interest were disclosed.

References

1. Watanabe K, Hasegawa Y, Yamashita H, Shimizu K, Ding Y, Abe M, Ohta H, Imagawa K, Hojo K, Maki H, Sonoda H, Sato Y (2004) Vasohibin as an endothelium-derived negative feedback regulator of angiogenesis. J Clin Invest 114:898–907.
2. Shibuya T, Watanabe K, Yamashita H, Shimizu K, Miyashita H, Abe M, Moriya T, Ohta H, Sonoda H, Shimosegawa T, Tabayashi K, Sato Y (2006) Isolation and characterization of vasohibin-2 as a homologue of VEGF-inducible endothelium-derived angiogenesis inhibitor vasohibin. Arterioscler Thromb Vasc Biol 26: 1051–1057.
3. Takahashi Y, Koyanagi T, Suzuki Y, Saga Y, Kanomata N, Moriya T, Suzuki M, Sato Y (2012) Vasohibin-2 expressed in human serous ovarian adenocarcinoma accelerates tumor growth by promoting angiogenesis. Mol Cancer Res 10:1135–1146.
4. Kimura H, Miyashita H, Suzuki Y, Kobayashi M, Watanabe K, Sonoda H, Ohta H, Fujiwara T, Shimosegawa T, Sato Y (2009) Distinctive localization and opposed roles of vasohibin-1 and vasohibin-2 in the regulation of angiogenesis. Blood 113:4810–4818.
5. Shen Z, Kauttu T, Seppanen H, Vainionpaa S, Ye Y, Wang S, Mustonen H, Puolakkainen P (2012) Vasohibin-1 and vasohibin-2 expression in gastric cancer cells and TAMs. Med Oncol 29:2718–2726.
6. Xue X, Gao W, Sun B, Xu Y, Han B, Wang F, Zhang Y, Sun J, Wei J, Lu Z, Zhu Y, Sato Y, Sekido Y, Miao Y, Kondo Y (2013) Vasohibin 2 is transcriptionally activated and promotes angiogenesis in hepatocellular carcinoma. Oncogene 32:1724–1734.
7. Koyanagi T, Saga Y, Takahashi Y, Suzuki Y, Suzuki M, Sato Y (2013) Downregulation of vasohibin-2, a novel angiogenesis regulator, suppresses tumor growth by inhibiting angiogenesis in endometrial cancer cells. Oncol Lett 5:1058–1062.
8. Kitahara S, Suzuki Y, Morishima M, Yoshii A, Kikuta S, Shimizu K, Morikawa S, Sato Y, Ezaki T (2014) Vasohibin-2 modulates tumor onset in the gastrointestinal tract by normalizing tumor angiogenesis. Mol Cancer 13:99.
9. Tu M, Liu X, Han B, Ge Q, Li Z, Lu Z, Wei J, Song G, Cai B, Lv N, Jiang K, Wang S, Miao Y, Gao W (2014) Vasohibin2 promotes proliferation in human breast cancer cells via upregulation of fibroblast growth factor2 and growth/differentiation factor15 expression. Mol Med Rep 10:663–669.
10. Kim JC, Kim KT, Park JT, Kim HJ, Sato Y, Kim HS (2015) Expression of vasohibin-2 in pancreatic ductal adenocarcinoma promotes tumor progression and is associated with a poor clinical outcome. Hepatogastroenterology 62:251–256.
11. Sato Y (2013) The vasohibin family: a novel family for angiogenesis regulation. J Biochem 153:5–11.
12. Brandizzi F, Barlowe C (2013) Organization of the ER-Golgi interface for membrane traffic control. Nat Rev Mol Cell Biol 14:382–392.
13. Nickel W, Rabouille C (2009) Mechanisms of regulated unconventional protein secretion. Nat Rev Mol Cell Biol 10:148–155.
14. Rubartelli A, Cozzolino F, Talio M, Sitia R (1990) A novel secretory pathway for interleukin-1 beta, a protein lacking a signal sequence. EMBO J 9:1503–1510.
15. Dupont N, Jiang S, Pilli M, Ornatowski W, Bhattacharya D, Deretic V (2011) Autophagy-based unconventional secretory pathway for extracellular delivery of IL-1beta. EMBO J 30:4701–4711.
16. Kakkar R, Hei H, Dobner S, Lee RT (2012) Interleukin 33 as a mechanically responsive cytokine secreted by living cells. J Biol Chem 287:6941–6948.
17. Duran JM, Anjard C, Stefan C, Loomis WF, Malhotra V (2010) Unconventional secretion of Acb1 is mediated by autophagosomes. J Cell Biol 188:527–536.
18. Manjithaya R, Anjard C, Loomis WF, Subramani S (2010) Unconventional secretion of Pichia pastoris Acb1 is dependent on GRASP protein, peroxisomal functions, and autophagosome formation. J Cell Biol 188:537–546.
19. Malhotra V (2013) Unconventional protein secretion: an evolving mechanism. EMBO J 32:1660–1664.
20. Zemskov EA, Mikhailenko I, Hsia RC, Zaritskaya L, Belkin AM (2011) Unconventional secretion of tissue transglutaminase involves phospholipid-dependent delivery into recycling endosomes. PLoS One 6:e19414.
21. Hughes RC (1999) Secretion of the galectin family of mammalian carbohydrate-binding proteins. Biochim Biophys Acta 1473:172–185.
22. Simons D, Grieb G, Hristov M, Pallua N, Weber C, Bernhagen J, Steffens G (2011) Hypoxia-induced endothelial secretion of macrophage migration inhibitory factor and role in endothelial progenitor cell recruitment. J Cell Mol Med 15:668–678.
23. Glebov K, Schutze S, Walter J (2011) Functional relevance of a novel SlyX motif in non-conventional secretion of insulin-degrading enzyme. J Biol Chem 286: 22711–22715.

24. Ding Y, Wang J, Wang J, Stierhof YD, Robinson DG, Jiang L (2012) Unconventional protein secretion. Trends Plant Sci 17:606–615.
25. Nickel W (2010) Pathways of unconventional protein secretion. Curr Opin Biotechnol 21:621–626.
26. Suzuki Y, Kobayashi M, Miyashita H, Ohta H, Sonoda H, Sato Y (2010) Isolation of a small vasohibin-binding protein (SVBP) and its role in vasohibin secretion. J Cell Sci 123:3094–3101.
27. Pedelacq JD, Cabantous S, Tran T, Terwilliger TC, Waldo GS (2006) Engineering and characterization of a superfolder green fluorescent protein. Nat Biotechnol 24:79–88.
28. Loening AM, Dragulescu-Andrasi A, Gambhir SS (2010) A red-shifted Renilla luciferase for transient reporter-gene expression. Nat Methods 7:5–6.
29. Horie S, Suzuki Y, Kobayashi M, Kadonosono T, Kondoh S, Kodama T, Sato Y (2016) Distinctive role of vasohibin-1A and its splicing variant vasohibin-1B in tumor angiogenesis. Cancer Gene Ther 23:133–141.
30. Lam AJ, St-Pierre F, Gong Y, Marshall JD, Cranfill PJ, Baird MA, McKeown MR, Wiedenmann J, Davidson MW, Schnitzer MJ, Tsien RY, Lin MZ (2012) Improving FRET dynamic range with bright green and red fluorescent proteins. Nat Methods 9:1005–1012.
31. Larkin MA, Blackshields G, Brown NP, Chenna R, McGettigan PA, McWilliam H, Valentin F, Wallace IM, Wilm A, Lopez R, Thompson JD, Gibson TJ, Higgins DG (2007) Clustal W and Clustal X version 2.0. Bioinformatics 23:2947–2948.
32. Jones DT (1999) Protein secondary structure prediction based on position-specific scoring matrices. J Mol Biol 292:195–202.
33. Morris MC, Deshayes S, Heitz F, Divita G (2008) Cell-penetrating peptides: from molecular mechanisms to therapeutics. Biol Cell 100:201–217.
34. Vorobyov I, Allen TW (2011) On the role of anionic lipids in charged protein interactions with membranes. Biochim Biophys Acta 1808:1673–1683.
35. Sonoda H, Ohta H, Watanabe K, Yamashita H, Kimura H, Sato Y (2006) Multiple processing forms and their biological activities of a novel angiogenesis inhibitor vasohibin. Biochem Biophys Res Commun 342:640–646.
36. Keller M, Ruegg A, Werner S, Beer HD (2008) Active caspase-1 is a regulator of unconventional protein secretion. Cell 132:818–831.
37. Xiang Y, Wang Y (2011) New components of the Golgi matrix. Cell Tissue Res 344:365–379.
38. Witkos TM, Lowe M (2015) The Golgin family of coiled-coil tethering proteins. Front Cell Dev Biol 3:86.
39. McNaughton BR, Cronican JJ, Thompson DB, Liu DR (2009) Mammalian cell penetration, siRNA transfection, and DNA transfection by supercharged proteins. Proc Natl Acad Sci U S A 106:6111–6116.
40. Hartenstein V (2006) Blood cells and blood cell development in the animal kingdom. Annu Rev Cell Dev Biol 22:677–712.
41. Shimizu K, Watanabe K, Yamashita H, Abe M, Yoshimatsu H, Ohta H, Sonoda H, Sato Y (2005) Gene regulation of a novel angiogenesis inhibitor, vasohibin, in endothelial cells. Biochem Biophys Res Commun 327:700–706.
42. Sanchez-Pulido L, Ponting CP (2016) Vasohibins: new transglutaminase-like cysteine proteases possessing a non-canonical Cys-His-Ser catalytic triad. Bioinformatics 32:1441–1445.